Aleksei Orlov, Amit Gefen,
How influential is the stiffness of the foam dressing on soft tissue loads in negative pressure wound therapy?
Medical Engineering & Physics, 2021 https://doi.org/10.1016/j.medengphy.2021.02.001.

Manuscript Number **MEP-D-20-00583** (Revision) January 13th, 2020

How influential is the stiffness of the foam dressing on soft tissue loads in negative pressure wound therapy?

Aleksei Orlov, Amit Gefen*

Department of Biomedical Engineering, Faculty of Engineering,
Tel Aviv University, Tel Aviv, Israel

***Corresponding author:**

Prof. Amit Gefen
The Herbert J. Berman Chair in Vascular Bioengineering
Department of Biomedical Engineering
Faculty of Engineering
Tel Aviv University
Tel Aviv 6997801, Israel
Tel: +972-3-6408093
Fax: +972-3-6405845
E-mail: gefen@tauex.tau.ac.il

***Keywords*:**

Wound care; tissue repair and regeneration; pressure ulcer; diabetic foot ulcer; biomechanical model.

Submitted to the *Medical Engineering & Physics*

Abstract

Negative pressure wound therapy (NPWT) is an established adjunctive modality for treatment of both acute and chronic wounds. However, little is known about the optimal settings and combination of treatment parameters and importantly, how these translate to target tissue strains and stresses that would result the fastest healing and buildup of good-quality tissues. Here we have used a three-dimensional open wound computational (finite element) model that contains viscoelastic skin, adipose and skeletal muscle tissue components for determining the states of tissue strains and stresses in and around the wound when subjected to NPWT with foam dressings of varying stiffnesses. We found that the skin strain state is considerably more sensitive to the pressure level than to the stiffness of the foam dressing within a 8.25 to 99 kPa range which covers the current industry standard. Accordingly, peri-wound skin strains and stresses which stimulate cell proliferation/migration and angiogenesis and thereby, healing of the wound, can be more effectively controlled by adjusting the pressure level than by varying the stiffness of the foam dressing.

1. Introduction

Negative pressure wound therapy (NPWT), a wound care technology employing a suction pump with tubing connected to a foam dressing for removal of excess exudates and promotion of healing, is currently one of the most popular treatment approaches. Since its introduction in the 1990's, NPWT is considered a mainstream procedure for management of acute, chronic and complex wounds in both acute and outpatient care [1]. Today, NPWT is used for treating a variety of wound types, including those associated with orthopaedic and soft tissue traumas, burns, surgical incisions, pressure ulcers and diabetic foot ulcers [2–7].

Application of NPWT induces physical and biological responses at the macroscopic and microscopic scales within the wound-bed and also, in peri-wound tissues [8–10]. There are multiple mechanisms of action that have been proposed in the literature as contributing to the efficacy of NPWT. The fluid management feature of NPWT forms a controlled moist environment, drains excessive exudates and, thereby reduces the edema, which reliefs tissue loads and helps to contract the wound edges. The NPWT – induced deformations, are also beneficial for mechanically stimulating the wound bed and enhancing the blood flow around the wound, which supports further angiogenesis and the formation of granulation tissue [11–13].

Macro-strain is the physical wound shrinkage that can be observed immediately after application of a NPWT device, as the wound edges are pulled together [10,14]. At the tissue microscale, these macro-level deformations are associated with mechanobiological stimulation of keratinocytes, fibroblasts, leukocytes, endothelial and other epithelial cells that play a role in epithelization of the wound-bed and later, in tissue repair and regeneration through fibrosis and angiogenesis [15]. Exposure of these cells to deformations, either static or dynamic, activates mechanoreceptors in their plasma membrane and triggers collective proliferation and/or migratory activities [13]. Accordingly, understanding the multi-scale mechanobiology of NPWT is pivotal for improving this wound care technology further. For example, in our recently published work employing an in vitro cell stimulation system developed to simulate the cell-scale microenvironment induced by NPWT, we have identified specific micro-deformation

levels and wave shapes that promote collective migration of fibroblasts towards damage sites in cultures [16].

To date, the overall lack of basic science research into the mechanisms of action and in particular, the mechanobiology of NPWT is manifested in a large variety of NPWT devices with different operating modes. The NPWT protocols, programmed options and adjustments of parameters are set in practice, based on clinical judgment and experience which may be subjective and influenced by the manufacturer agenda and commercial considerations. Deeper understanding of the mechanobiology of NPWT will lead to a better-informed device and/or protocol design process, more focus on objective performances and less confusion in this market, which will ultimately improve wound care outcomes. Specifically, for improving the design of devices and protocols and for tailoring treatment sessions to individual patients so that reproducible and consistent clinical outcomes are achieved, it is crucial to understand how NPWT affects soft tissues from a biomechanical perspective.

Computational finite element (FE) modelling is a powerful tool for investigating and comparing the efficacies of medical devices, including those in the wound care arena. Very little biomechanical modelling work has been published in the context of NPWT and in particular, regarding magnitudes and distributions of the mechanical loads that form in the wound-bed and peri-wound tissues under the effect of these devices. The pioneering work of Saxena and colleagues [17] described a two-dimensional (2D), linear-elastic FE model of the biomechanical interactions between a foam dressing and a wound surface during application of sub-atmospheric pressure through the porous foam. In a later study of Wilkes et al. [18], they extended the modelling to a 3D geometry of the dressing-wound interaction at the meso-scale and investigated the effects of the dressing type (focusing on open cell foam versus gauze), sub-atmospheric pressure (0-200 mmHg) and tissue mechanical properties on the micro-deformations in the wound-bed. However, their work did not consider viscoelastic tissue behavior or the wound shape (as their model geometry described the meso-scale). In further work, Wilkes et al. [19] up-scaled their analyses to the macro-level, investigating a closed-incision surgical wound managed through NPWT, however, they only considered a 2D cross-sectional plane through the incision, which ignores the out-of-plane biomechanical interactions. Similarly, Loveluck et al. [20]

developed a thin-slice FE model of a surgical incision treated by a single-use NPWT device that was limited to in-plane analysis of tissue loads. Both works simplified soft tissue behaviors as being hyperelastic and neglected any viscoelastic effects which are fundamental and highly influential in the context of NPWT. Our group were the first to introduce viscoelastic soft tissue behavior to the NPWT modelling framework, which is essential in order to account for stress relaxation phenomena that occur in the affected tissues during application of either static or dynamic NPWT [21]. We further considered additional realistic and physiologically/clinically-relevant features, including a non-circular wound geometry and distinct epidermis versus dermis layers of skin (as opposed to the simplified bulk skin layer used in previous works) and have subjected the simulated wound to time-dependent negative pressure levels applied through a foam dressing [21].

Our present study builds upon our aforementioned published modelling work [21]. Specifically, we utilize a 3D viscoelastic, large-deformation, open wound FE model for determining the states of tissue strains and stresses during application of NPWT, with a present focus on the influence of the stiffness properties of the foam dressing that covers the wound in this therapeutic method. Our objective has been to determine whether altering the stiffness of the foam dressing is a valid and effective route for modulating the tissue loads generated by the negative pressures, e.g. for different healing stages or for personalized medicine.

2. Methods

2.1 Geometry of the model

We have modelled a deep skin defect with elliptical dimensions of 120×70 mm (length × width) that extends into subepidermal adipose tissue (Fig. 1a) and represents an open wound, such as a category III pressure ulcer, which would be treated by NPWT without primary suture closure. The model comprised of four soft tissue layers: epidermis, dermis, adipose and underlying skeletal muscle with thicknesses of 1,2,8 and 12 mm, respectively [22] (Fig. 1a). A NPWT foam dressing has been modelled as a single rectangular layer of foam with dimensions of 145×95×15 mm (length × width × height), where the longest aspect of the foam aligned with the widest dimension of the wound, so that the foam dressing covered the entire wound-bed and peri-wound skin (Fig. 1b). The overall model

dimensions (i.e. the geometrical model domain) were 500×500×23 mm (length × width × height).

The above geometry of the model domain (Fig. 1a) was created using the Scan-IP module of the Simpleware® software package [23].

2.2 Boundary, contact and loading conditions

The side faces of the model were fixed for all translations and rotations to consider the continuum interactions with tissues outside the model domain, whereas the superior (skin side) and inferior surfaces of the model were allowed to move in response to the applied negative pressures. The contacts between tissue layers (epidermis-dermis, dermis-adipose and adipose-muscle) were all set as "tie" ('no-slip condition') (Fig. 1a; bottom frame). The foam dressing was likewise modeled as being adhered to the skin (i.e. no slippage allowed between the foam and skin) (Fig. 1b). Negative pressure was simulated as hydrostatic compression applied to all 6 surfaces of the foam dressing (the superior aspect, inferior aspect and the 4 sides).

2.3 Finite element simulations and outcome measures

Each of the aforementioned soft tissues was assumed to behave as a viscoelastic solid. The hyperelastic component of this viscoelastic behavior was considered to be Neo-Hookean [21,24,25] with a strain energy density function W:

$$W = \frac{\mu}{2}(I_1 - 3) - \mu \ln J + \frac{\lambda}{2}(\ln J)^2 \qquad \text{(Eq.1)}$$

where λ and μ are Lame's first and second parameters, respectively, I_1 being the first invariant of the right Cauchy-Green deformation tensor and J is the determinant of the deformation gradient tensor. The viscous components of the individual tissue layer behavior was simulated using a Prony-series of stress relaxation functions:

$$G(t) = 1 + \sum_{i=1}^{N} \gamma_i e^{-t/\tau_i} \qquad \text{(Eq.2)}$$

where γ_i, τ_i, and i=1, 2, … N, are the tissue-specific material constants. For efficiency of the computations and reduction of the number of parameters, we have selected the minimal N=2, which yields short-term and long-term viscoelastic relaxation time constants for each

soft tissue type, τ_1 and τ_2, respectively. The λ and μ, τ_1 and τ_1, and γ_1 and γ_2 parameter values for each tissue type have been selected based on published literature as detailed in Table 1. To determine the NPWT foam dressing properties, we have conducted experimental testing of commercial NPWT foam specimens using an electromechanical testing machine (Instron® Series 5944, Instron Co., MA, USA) following the relevant testing standard ASTM D3574-11[26]. We have tested flexible cellular foam specimens compressed at a deformation rate of 50 ± 5 mm/min and converted the compressive force displacement data to stress-strain curves as per the above testing standard. Considering the tested foam as homogenous, isotropic and hyperelastic materials, we have used the ABAQUS software suite (Dassault Systems, Vélizy-Villacoublay, France) to determine the λ and μ parameters of the tested foams, and the corresponding representative values are also specified in Table 1.

The action of the NPWT was simulated as static negative pressure, delivered through the foam dressing (Fig. 1b) at a range of 10 to 175 mmHg, which covers the whole range of the commercially available static NPWT devices (including the single-use devices). In order to test the effects of the stiffness of the applied foam dressing on the calculated tissue strain and stress data, we have made the foam up to one order of magnitude stiffer or, up to one order of magnitude softer with respect to the current industry standard (i.e. elastic modulus E of 16.5 kPa; Table 1), which yielded a foam stiffness range of E = 8.25 to 99 kPa [27,28].

The aforementioned model geometry was meshed using the Scan-IP module of Simpleware® software [23]. The meshing was performed semi-automatically, i.e. with manual refinements near the borders of the wound-bed and the foam dressing (Fig. 1b). All the mesh elements were tetrahedral; the numbers of elements for each tissue type and the foam dressing are further listed in Table 1. All the FE analyses were conducted using the FEBio Software suite [24].

The model was analyzed for the Green-Lagrange strains and Cauchy stresses in adipose tissue at the center of the wound-bed and at the peri-wound skin. Accordingly, two regions of interest (ROIs) were defined, a disc with diameter of 2 cm and depth of 7 mm at the center of the wound-bed and a second disc of identical size, located 7 cm laterally from the center of the wound-bed on the axis of the narrower wound width (i.e. the shorter axis of

the ellipse-shape wound). The latter ROI therefore contained the full thicknesses of both the epidermis and dermis layers of the peri-wound skin.

Outcome measures for data analysis included the distributions of effective strain and stress magnitudes at the model domain with focus on the strain/stress values in tissues at the two ROIs with respect to the NPWT pressure level and as function of the stiffness of the NPWT foam dressing. Since denser foam dressings with smaller pores would generally require a higher negative pressure level to collapse compared to less dense foams with larger pores [29], we have conducted further analyses to determine the sensitivity of the strain/stress values in tissues at the two ROIs to the foam stiffness within the 75-125 mmHg pressure range.

3. Results

The highest tissue strains occurred at the simulated wound-bed (Fig. 2a) whereas tissue stresses maximized in peri-wound skin. At the margins of the wound, stress values were highest at the epidermis, then in the dermis and lowest in adipose tissue, at approximate ratios of 1:2:10, respectively (Fig. 2b).

An increase in the negative pressure level within the 10-175 mmHg range caused both the effective tissue strain and stress values to rise. Specifically, for the above pressure range, strains in the wound-bed increased from 3% to 43% and strains in peri-wound skin increased from 0.3% to 3%; the corresponding (effective) wound-bed and peri-wound tissue stresses increased from 0.3 kPa to 5 kPa and from 96 kPa to 1250 kPa, respectively (Figs. 3,4). While the median tissue strain and stress values increased monotonically with the rise in pressure levels, the variation (standard deviation of strain/stress data around the mean value) widened considerably as the pressure levels grew, particularly with regards to strains in peri-wound skin. Specifically, as the pressure levels increased within the 10-175 mmHg range, the coefficient of variation (CV) for the wound-bed outcome measures increased from 73% to 86% for strains and from 72% to 89% for stress data. Likewise, for peri-wound skin (i.e. epidermis and dermis pooled), the CV increased from 71% to 169% for strains and from 116% to 124% for stresses.

The stiffness of the foam dressing only had a mild effect on strain and stress levels in the wound-bed. Moreover, the foam stiffness had a negligible effect on peri-wound strain and

stress levels, which is in stark contrast to the influence of the negative pressure intensity on these outcome measures (Figs. 5-7). Specifically, for a variation in the elastic modulus of the foam dressing within an order of magnitude around the industry standard (for a dry dressing), i.e. from 8.25 to 99 kPa where the negative pressure value was set to the midrange value of 100 mmHg, wound-bed loads increased in the range of 20-30% for strains and 2.25-3.25 kPa for stresses (Figs. 5-7). Furthermore, our sensitivity analyses concerning the effects of negative pressure variations on tissue strains/stresses demonstrated that for the peri-wound skin (epidermis and dermis), the mean effective strain and stress values only varied negligibly with the foam stiffness for each certain negative pressure level within the 75-125 mmHg range (Figs. 6,7). Importantly, these peri-wound skin strain and stress data remained nearly unchanged for the studied variation in the foam stiffnesses: Epidermis and dermis strains were 1.6 and 2%, respectively, and remained at approximately those values within a ±0.15% strain interval regardless of the foam dressing stiffness value (Figs. 6,7). Consistent with the above, epidermis and dermis stresses were 1438 kPa and 178 kPa, respectively, and likewise did not change by more than ± 15 kPa for the entire studied range of foam stiffnesses.

Our present computational simulation data therefore demonstrated that the strain and stress states in peri-wound skin are considerably more sensitive to the pressure level set in the NPWT device/protocol (Figs. 3b, 4b) than to the stiffness of the foam dressing (Figs. 5b, 6b). Stiffer and softer foam dressings over an order of magnitude around the mean industry standard (for a dry dressing) yielded indistinguishable strains and stresses, particularly in peri-wound skin which, from a biological perspective, is the reservoir for healing, being the source for immune and tissue-repairing cells, as well as of vascular supply (Figs. 5b, 6b).

4. Discussion

Negative pressure wound therapy is an established adjunctive modality for treatment of both acute and chronic wounds [14,30–32]. Yet, level-1 clinical evidence (including randomized controlled trials, RCTs and systematic reviews) reveals that clinical outcomes differ substantially across populations, wound types and etiologies, clinical settings, protocols, devices and treatment parameters [33–39]. A recent systematic review of 93

RCTs specifically stated that trial findings are inconsistent with respect to clinically relevant endpoints, such as the incidence of, or the time to complete wound closure [37].

The above mixed clinical outcomes must connect with the overall poor science and knowledge regarding optimal protocols, device settings and combination of treatment parameters. What is optimal for wave-shapes of the negative pressure, pressure magnitudes and, the frequency of pressure changes is currently unknown. Importantly, how negative pressure wave-shapes and magnitudes translate to target soft tissue strains and stresses that would result the fastest healing, buildup of good-quality tissues and no keloid scarring is yet to be discovered [21,40,41]. Work is underway in our laboratory in this regard, focusing on development of an experimental-computational modelling framework for better understanding of the mechanobiology of cells and tissues at peri-wound and wound-bed sites subjected to NPWT [16].

The present work has made significant progress in modelling NPWT, as both the Wilkes et al. [19] and the Loveluck et al. [20] previous NPWT models were substantially more simplified than what we have achieved here. Specifically, the Loveluck model was a thin-slice model and the Wilkes model was a two-dimensional cross-section (i.e. with no thickness assigned to it). This implies that the Loveluck and the Wilkes models did not consider out-of-plane forces applied by the NPWT and tissue reaction forces to these out-of-plane forces. Furthermore, the tissue material behaviors in both the Loveluck and Wilkes works are considered to behave according to an Ogden hyperelastic strain energy function and therefore, they are time-independent (which is again an oversimplifying assumption). Contrarily, in the present study, we have considered the viscoelasticity (i.e. the stress relaxation phenomena) in all soft tissues (Table 1). Our consideration of full three-dimensionality of the wound-bed and the entire geometrical domain as well as the viscoelastic soft tissue behaviors are key features in the progress made in this present NPWT modelling framework, which is substantially more advanced and realistic with respect to the Wilkes [19] and Loveluck [20] papers.

In the above context, the present work was aimed at developing a computational FE modelling framework where we have developed a 3D, open wound model and utilized it for determining the states of tissue strains and stresses around the aforementioned wound, when subjected to NPWT. In particular, the present model facilitated studies of the

influence of the stiffness properties of the foam dressings that are generically being used in NPWT, on the dynamic strain and stress states generated in the wound-bed and at the peri-wound. Of note, it is important to determine tissue stresses in both locations as intact skin is stiffer than wound-bed tissues, indicating that greater deformations are expected in the wound-bed [21]. It is not surprising therefore that the higher stresses are associated with adipose tissue. Accordingly, NPWT which is applied externally to the body surface, is expected to form greater tissue stresses at peri-wound (intact skin) regions than in the wound-bed, which is an important principle not previously underpinned in the literature. In fact, the applied negative pressure directly forms high stress sites at the skin surface, which then diffuse to deeper dermal layers and to subcutaneous fat. As noted in our previously published work, the NPWT affects different tissue layers at various extents, depending on the mass and stiffness of each such layer [21].

The most important and perhaps unexpected finding of the present study is that the peri-wound skin stresses, which are considered to be physiologically important for stimulating healing by NPWT (e.g. through angiogenesis, proliferation and migration of phagocyte and fibroblast cells, and synthesis of collagen [8,9,42,43]) were only slightly affected by the stiffness of the foam dressing (around an order of magnitude with respect to measured commercial product stiffnesses) (Figures 5b, 6b).

While we did not model direct relations between exudate fluid retention and the stiffness of the foam dressing, we surmise that these effects are inherently incorporated in the wide range of variation of foam stiffness properties that had already been considered in the present sensitivity analyses (8.25 to 99 kPa, which is an order of magnitude difference between the different tested foam stiffness levels). Based on the work of Brown and Pearcy [44], who measured the effect of water content on the stiffness of open-cell polyurethane foams which are the primary NPWT dressing material, we deduce that stiffness changes caused by wetness will be less than 5-fold, which is well contained within the range of foam stiffnesses tested here (for which no substantial effect of the foam stiffness on the peri-wound skin strain-stress states has been shown) [44]. As with any modelling work, the present study involved assumptions and limitations that need to be reviewed for completeness. The stiffness and thickness properties of the soft tissue layers assumed uniform, whereas in reality they are not, and the wound itself was simulated to be axi-

symmetrical, which rarely occurs in the real-world. Nevertheless, the above simplifications were helpful in describing a more 'generic' wound shape and tissue structure, which assisted in focusing on the influence of the foam dressing stiffness on tissue stresses, being the primary purpose of this work. Non-uniformities in tissue stiffness or thickness, or shape asymmetries of the wound would like contribute to the intensities of the formed tissue stress concentrations and make them more irregular. This, in turn, would have caused the results to be more difficult to interpret systematically, which justifies the uniform tissue thickness and wound shape choices made here for the specific study objectives.

In conclusion, we have developed an FE modelling framework of NPWT treatments of an open wound, which indicates that the strain-stress states induced be the NPWT system at peri-wound tissues can be more effectively controlled by adjusting the pressure level than by varying the stiffness of the foam dressing. Whilst peri-wound skin is the main biological reservoir for wound healing, the effective approach to control its level of stimulation is to regulate the NPWT pressure level. By leading to this conclusion through a sensitivity analysis approach, our present modelling work contributes to better understanding of the mechanobiological effects of NPWT and how this technology could be potentially improved in terms of controlling the strains and stresses in the wound-bed and peri-wound skin.

Acknowlegments

This project has received funding from the European Union's Horizon 2020 research and innovation programme under the Marie Skłodowska-Curie grant agreement No. 811965 (STINTS). This work was also partially supported by the Israeli Ministry of Science & Technology (Medical Devices Program Grant no. 3-17421, awarded to Professor Amit Gefen in 2020).

Competing interests: None declared

Ethical approval: Not required

References

[1] Bobkiewicz A, Banasiewicz T, Ledwosiński W, Drews M. Medical terminology associated with Negative Pressure Wound Therapy (NPWT). Understanding and misunderstanding in the field of NPWT. Negat Press Wound Ther 2014;1:69-73.

[2] Bollero D, Carnino R, Risso D, Gangemi EN, Stella M. Acute complex traumas of the lower limbs: a modern reconstructive approach with negative pressure therapy. Wound Repair Regen 2007;15:589-94. https://doi.org/10.1111/j.1524-475X.2007.00267.x.

[3] Stannard JP, Robinson JT, Anderson ER, McGwin G, Volgas DA, Alonso JE. Negative pressure wound therapy to treat hematomas and surgical incisions following high-energy trauma. J Trauma Inj Infect Crit Care 2006;60:1301-6. https://doi.org/10.1097/01.ta.0000195996.73186.2e.

[4] Scherer LA, Shiver S, Chang M, Wayne Meredith J, Owings JT. The vacuum assisted closure device: A method of securing skin grafts and improving graft survival. Arch Surg 2002;137:930-4. https://doi.org/10.1001/archsurg.137.8.930.

[5] Armstrong DG, Lavery LA. Negative pressure wound therapy after partial diabetic foot amputation: A multicentre, randomised controlled trial. Lancet 2005;366:1704-10. https://doi.org/10.1016/S0140-6736(05)67695-7.

[6] Kamolz LP, Andel H, Haslik W, Winter W, Meissl G, Frey M. Use of subatmospheric pressure therapy to prevent burn wound progression in human: First experiences. Burns 2004;30:253-8. https://doi.org/10.1016/j.burns.2003.12.003.

[7] Gustafsson RI, Sjögren J, Ingemansson R. Deep sternal wound infection: A sternal-sparing technique with vacuum-assisted closure therapy. Ann Thorac Surg 2003;76:2048-53. https://doi.org/10.1016/S0003-4975(03)01337-7.

[8] Lalezari S, Lee CJ, Borovikova AA, Banyard DA, Paydar KZ, Wirth GA, et al. Deconstructing negative pressure wound therapy. Int Wound J 2017;14:649-57. https://doi.org/10.1111/iwj.12658.

[9] Huang C, Leavitt T, Bayer LR, Orgill DP. Effect of negative pressure wound therapy on wound healing. Curr Probl Surg 2014;51:301-31. https://doi.org/10.1067/j.cpsurg.2014.04.001.

[10] Orgill DP, Bayer LR. Negative pressure wound therapy: Past, present and future. Int

Wound J 2013;10:15-9. https://doi.org/10.1111/iwj.12170.

[11] Argenta LC, Morykwas MJ. Vacuum-assisted closure: A new method for wound control and treatment: Clinical experience. Ann Plast Surg 1997;38:563-77. https://doi.org/10.1097/00000637-199706000-00002.

[12] Morykwas MJ, Argenta LC, Shelton-Brown EI, McGuirt W. Vacuum-assisted closure: A new method for wound control and treatment: animal studies and basic foundation. Ann Plast Surg 1997;38:553-62. https://doi.org/10.1097/00000637-199706000-00001.

[13] Borgquist O, Gustafsson L, Ingemansson R, Malmsjö M. Micro- and Macromechanical effects on the wound bed of negative pressure wound therapy using gauze and foam. Ann Plast Surg 2010;64:789-93. https://doi.org/10.1097/SAP.0b013e3181ba578a.

[14] Apelqvist J, Willy C, Fagerdahl AM, Fraccalvieri M, Malmsjö M, Piaggesi A, et al. EWMA document: Negative pressure wound therapy: Overview, challenges and perspectives. J Wound Care 2017;26:S1-154. https://doi.org/10.12968/jowc.2017.26.Sup3.S1.

[15] Enyedi B, Niethammer P. Mechanisms of epithelial wound detection. Trends Cell Biol 2015;25:398-407. https://doi.org/10.1016/j.tcb.2015.02.007.

[16] Katzengold R, Orlov A, Gefen A. A novel system for dynamic stretching of cell cultures reveals the mechanobiology for delivering better negative pressure wound therapy. Biomech Model Mechanobiol 2020. https://doi.org/10.1007/s10237-020-01377-6.

[17] Saxena V, Hwang CW, Huang S, Eichbaum Q, Ingber D, Orgill DP. Vacuum-assisted closure: Microdeformations of wounds and cell proliferation. Plast Reconstr Surg 2004;114:1086-96. https://doi.org/10.1097/01.PRS.0000135330.51408.97.

[18] Wilkes R, Zhao Y, Kieswetter K, Haridas B. Effects of dressing type on 3D tissue microdeformations during negative pressure wound therapy: A computational study. J Biomech Eng 2009;131(3):031012. https://doi.org/10.1115/1.2947358.

[19] Wilkes RP, Kilpad D V., Zhao Y, Kazala R, McNulty A. Closed incision management with negative pressure wound therapy (CIM): Biomechanics. Surg Innov 2012;19:67-75. https://doi.org/10.1177/1553350611414920.

[20] Loveluck J, Copeland T, Hill J, Hunt A, Martin R. Biomechanical modeling of the forces applied to closed incisions during single-use negative pressure wound therapy. Eplasty 2016;16:e20.

[21] Katzengold R, Topaz M, Gefen A. Dynamic computational simulations for evaluating tissue loads applied by regulated negative pressure-assisted wound therapy (RNPT) system for treating large wounds. J Tissue Viability 2018;27:101-13. https://doi.org/10.1016/j.jtv.2017.10.004.

[22] Lee Y, Hwang K. Skin thickness of Korean adults. Surg Radiol Anat 2002;24:183-9. https://doi.org/10.1007/s00276-002-0034-5.

[23] 3D Image Segmentation Software | Simpleware ScanIP n.d. https://www.synopsys.com/simpleware/software/scanip.html (accessed January 11, 2021).

[24] FEBio - Musculoskeletal Research Laboratories n.d. https://mrl.sci.utah.edu/software/febio/ (accessed January 11, 2021).

[25] Hendriks FM, Brokken D, Oomens CWJ, Bader DL, Baaijens FPT. The relative contributions of different skin layers to the mechanical behavior of human skin in vivo using suction experiments. Med Eng Phys 2006;28:259-66. https://doi.org/10.1016/j.medengphy.2005.07.001.

[26] D3574-11 AITS. Standard test methods for flexible cellular materials - Slab, bonded, and molded urethane foams. Am Soc Test Mater 2012;Designatio:1-29. https://doi.org/10.1520/D3574-11.2.

[27] Moore B, Jaglinski T, Stone DS, Lakes RS. On the bulk modulus of open cell foams. Cellular Polymers 2007;26(1):1-10. https://doi.org/10.1177/026248930702600101

[28] Wang YC, Ko CC, Huang YH. Viscoelastic properties of foam under hydrostatic pressure and uniaxial compression. Procedia Engineering 2013;67:397-403. https://doi.org/10.1016/j.proeng.2013.12.039.

[29] Sambasivam M, White R, Cutting K. Exploring the role of polyurethane and polyvinyl alcohol foams in wound care. Wound Healing Biomaterials 2016;2:251-260. https://doi.org/10.1016/B978-1-78242-456-7.00012-X.

[30] Anghel EL, Kim PJ. Negative-pressure wound therapy: A comprehensive review of the evidence. Plast Reconstr Surg 2016;138:129s-137s.

https://doi.org/10.1097/PRS.0000000000002645.

[31] Zwanenburg PR, Timmermans FW, Timmer AS, Middelkoop E, Tol BT, Lapid O, et al. A systematic review evaluating the influence of incisional negative pressure wound therapy on scarring. Wound Repair Regen 2020:wrr.12858. https://doi.org/10.1111/wrr.12858.

[32] Othman D. Negative pressure wound therapy literature review of efficacy, cost effectiveness, and impact on patients' quality of life in chronic wound management and its implementation in the United kingdom. Plast Surg Int 2012;2012:374398. https://doi.org/10.1155/2012/374398.

[33] Vikatmaa P, Juutilainen V, Kuukasjärvi P, Malmivaara A. Negative pressure wound therapy: A systematic review on effectiveness and safety. Eur J Vasc Endovasc Surg 2008;36:438-48. https://doi.org/10.1016/j.ejvs.2008.06.010.

[34] Älgå A, Haweizy R, Bashaireh K, Wong S, Lundgren KC, von Schreeb J, et al. Negative pressure wound therapy versus standard treatment in patients with acute conflict-related extremity wounds: a pragmatic, multisite, randomised controlled trial. Lancet Glob Heal 2020;8:e423-9. https://doi.org/10.1016/S2214-109X(19)30547-9.

[35] Peinemann F, Sauerland S. Negative-pressure wound therapy: Systematic review of randomized controlled trials. Dtsch Arztebl Int 2011;108:381-9. https://doi.org/10.3238/arztebl.2011.0381.

[36] Sexton F, Healy D, Keelan S, Alazzawi M, Naughton P. A systematic review and meta-analysis comparing the effectiveness of negative-pressure wound therapy to standard therapy in the prevention of complications after vascular surgery. Int J Surg 2020;76:94-100. https://doi.org/10.1016/j.ijsu.2020.02.037.

[37] Peinemann F, Labeit A. Negative pressure wound therapy: A systematic review of randomized controlled trials from 2000 to 2017. J Evid Based Med 2019;12:125-32. https://doi.org/10.1111/jebm.12324.

[38] Thomson CH. Negative pressure wound therapy: A review of efficacy in pressure ulcers. Wounds UK 2013;9:52-8.

[39] Webster J, Liu Z, Norman G, Dumville JC, Chiverton L, Scuffham P, et al. Negative pressure wound therapy for surgical wounds healing by primary closure. Cochrane

Database Syst Rev. 2019;26;3(3):CD009261. https://doi.org/10.1002/14651858.CD009261.pub4.

[40] Ahearn C. Intermittent NPWT and Lower Negative Pressures - Exploring the disparity between science and current practice: A review. Ostomy Wound Manag 2009:22-8. https://www.o-wm.com/content/intermittent-npwt-and-lower-negative-pressures-exploring-disparity-between-science-and-cur (accessed January 11, 2021).

[41] Borgquist O, Ingemansson R, Malmsjö M. The effect of intermittent and variable negative pressure wound therapy on wound edge microvascular blood flow. Ostomy Wound Manage 2010;56(3):60-7. https://www.o-wm.com/content/the-effect-intermittent-and-variable-negative-pressure-wound-therapy-wound-edge-microvascula

[42] Wiegand C, White R. Microdeformation in wound healing. Wound Repair Regen 2013;21:793-9. https://doi.org/10.1111/wrr.12111.

[43] Mellott A, Zamierowski D, Andrews B. Negative pressure wound therapy in maxillofacial applications. Dent J 2016;4:30. https://doi.org/10.3390/dj4030030.

[44] Brown AM, Pearcy MJ. The effect of water content on the stiffness of seating foams. Prosthet Orthot Int 1986;10:149-52. https://doi.org/10.3109/03093648609164520.

[45] Xu F, Lu TJ. Chapter 3 Skin Biothermomechanics: Modeling and Experimental Characterization. Adv Appl Mech 2009;43:147-248. https://doi.org/10.1016/S0065-2156(09)43003-5.

Figure captions

Figure 1	Geometry and finite element mesh of the wound model: (a) The model with tissue and wound components. (b) The mesh around the wound-bed with the applied foam, showing an increased mesh density around the foam.
Figure 2	Distributions of the effective (a) strains and (b) stresses in the wound-bed and peri-wound tissues when a static negative pressure of 100 mmHg has been applied (the foam was hidden for clarity). The strains in (a) are shown through a cross-section (marked in the upper right frame).
Figure 3	Effective strain levels in (a) the wound-bed and (b) peri-wound skin for different negative pressure levels. Data are shown as box plots with medians represented by horizontal lines with the 75^{th} percentile at the top and the 25^{th} percentile at the bottom. The ends of the vertical lines (the "whiskers") in each such box indicate the minimum and maximum data values in the dataset. Variability in the plotted data is due to both the spatial and temporal variances as the computational data are collected from across the region of interest and while the tissues are responding viscoelastically to the applied negative pressure level.
Figure 4	Effective stress levels in (a) the wound-bed and (b) peri-wound skin for different negative pressure levels. Data are shown as box plots with medians represented by horizontal lines with the 75^{th} percentile at the top and the 25^{th} percentile at the bottom. The ends of the vertical lines (the "whiskers") in each such box indicate the minimum and maximum data values in the dataset. Variability in the plotted data is due to both the spatial and temporal variances as the computational data are collected from across the region of interest and while the tissues are responding viscoelastically to the applied negative pressure level.
Figure 5	Influence of the foam stiffness on wound-bed effective tissue (a) strain and (b) stress levels for static negative pressures of 75, 100 and 125 mmHg. Data are shown as box plots with medians represented by horizontal lines with the 75^{th} percentile at the top and the 25^{th} percentile at the bottom. The

	ends of the vertical lines (the "whiskers") in each such box indicate the minimum and maximum data values in the dataset. Variability in the plotted data is due to both the spatial and temporal variances as the computational data are collected from across the region of interest and while the tissues are responding viscoelastically to the applied negative pressure level.
Figure 6	Influence of the foam stiffness on peri-wound epidermal effective (a) strain and (b) stress levels for static negative pressures of 75, 100 and 125 mmHg. Data are shown as box plots with medians represented by horizontal lines with the 75^{th} percentile at the top and the 25^{th} percentile at the bottom. The ends of the vertical lines (the "whiskers") in each such box indicate the minimum and maximum data values in the dataset. Variability in the plotted data is due to both the spatial and temporal variances as the computational data are collected from across the region of interest and while the tissues are responding viscoelastically to the applied negative pressure level.
Figure 7	Influence of the foam stiffness on peri-wound dermal effective (a) strain and (b) stress levels for static negative pressures of 75, 100 and 125 mmHg. Data are shown as box plots with medians represented by horizontal lines with the 75^{th} percentile at the top and the 25^{th} percentile at the bottom. The ends of the vertical lines (the "whiskers") in each such box indicate the minimum and maximum data values in the dataset. Variability in the plotted data is due to both the spatial and temporal variances as the computational data are collected from across the region of interest and while the tissues are responding viscoelastically to the applied negative pressure level.

Table 1: Mechanical properties of the model components.

Model component	Lamé constants		Viscoelastic material parameters				Numbers of elements
	λ [MPa]	μ [MPa]	γ_1	τ_1 [s]	γ_2	τ_2 [s]	
Epidermis[a,b,c]	827	34.45	0.0864	0.212	0.214	4.68	133,157
Dermis[a,b,c]	82.7	3.44	0.0864	0.212	0.214	4.68	174,710
Adipose[a,b,c]	0.0827	0.0034	0.3988	2.04	0.12381	76.96	140,173
Muscle[c]	0.659	0.071	4.836	0.016	0.423	8.59	69,918
Foam[d]	0.051	0.0057	–	–	–	–	77,079

[a] Hendricks et al., 2006 [25]
[b] Xu and Lu, 2009 [45]
[c] Katzengold et al., 2018 [21]
[d] Measured in the present study

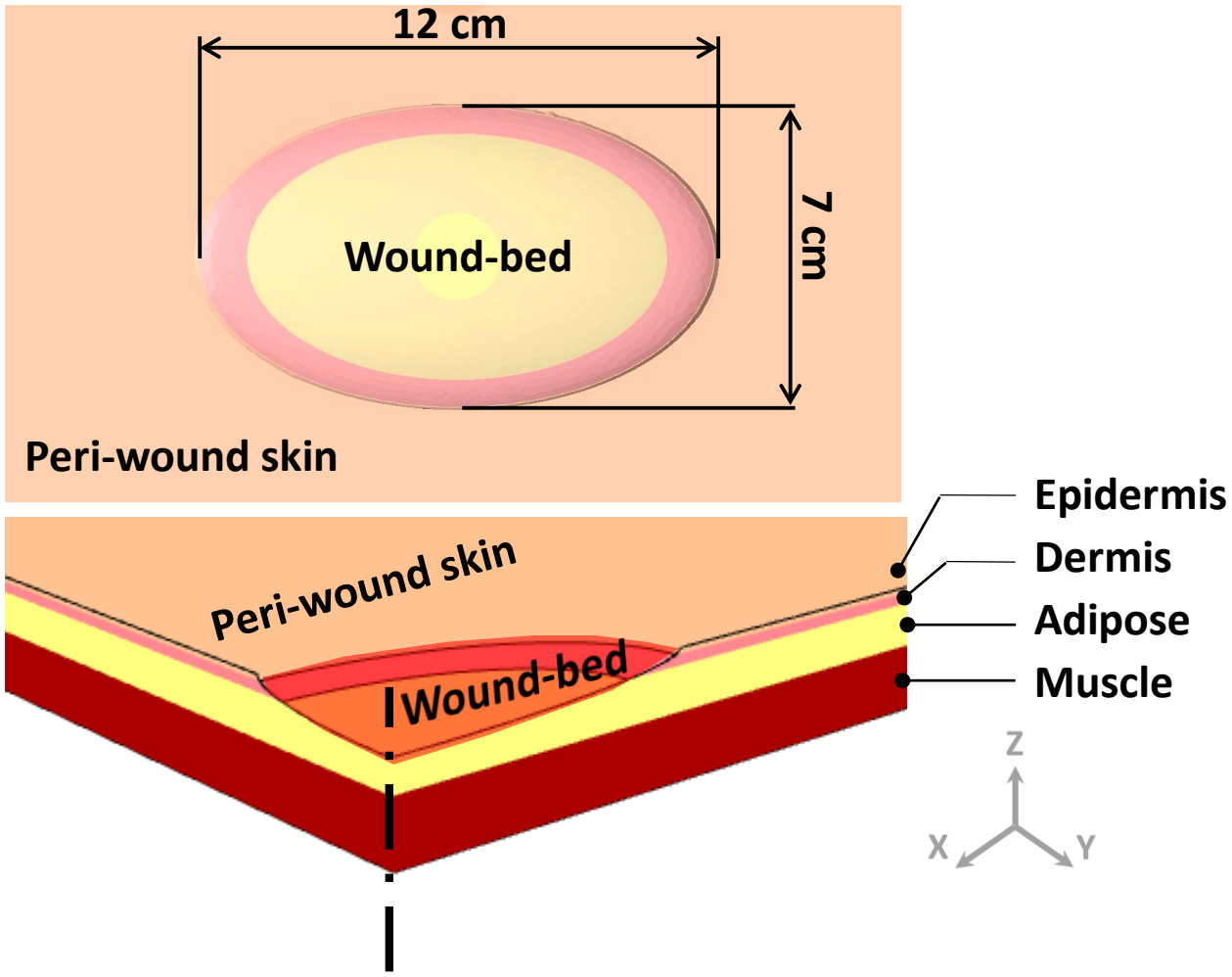
12 cm
7 cm
Wound-bed
Peri-wound skin
Peri-wound skin
Wound-bed
Epidermis
Dermis
Adipose
Muscle
Z
X
Y

(a)

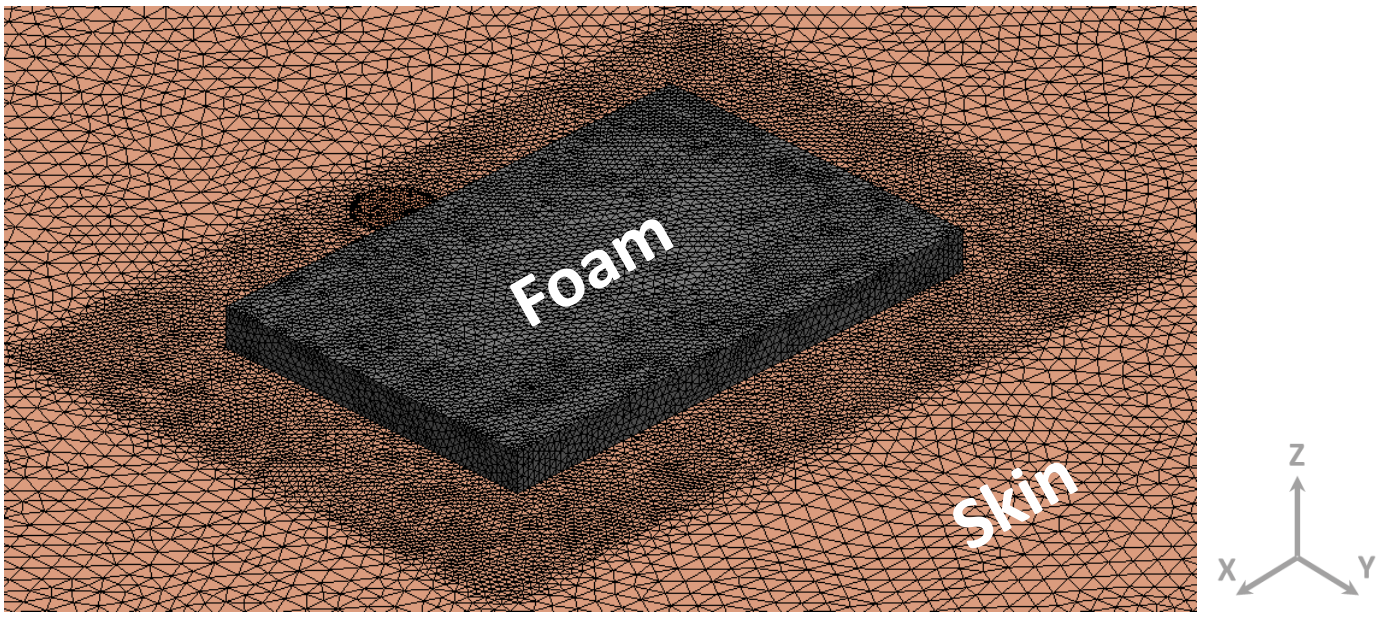
Foam
Skin
Z
X
Y

(b)

Figure 1

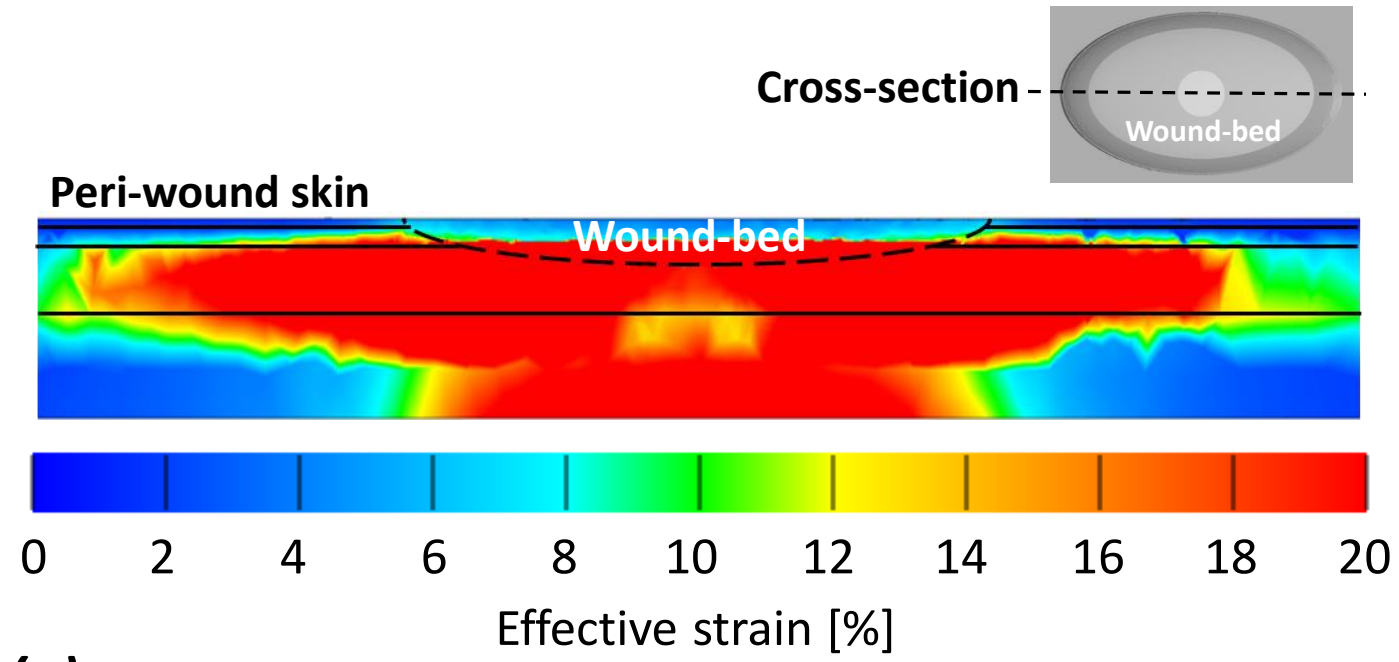
Cross-section
Wound-bed
Peri-wound skin
Wound-bed
0
2
4
6
8
10
12
14
16
18
20
Effective strain [%]

(a)

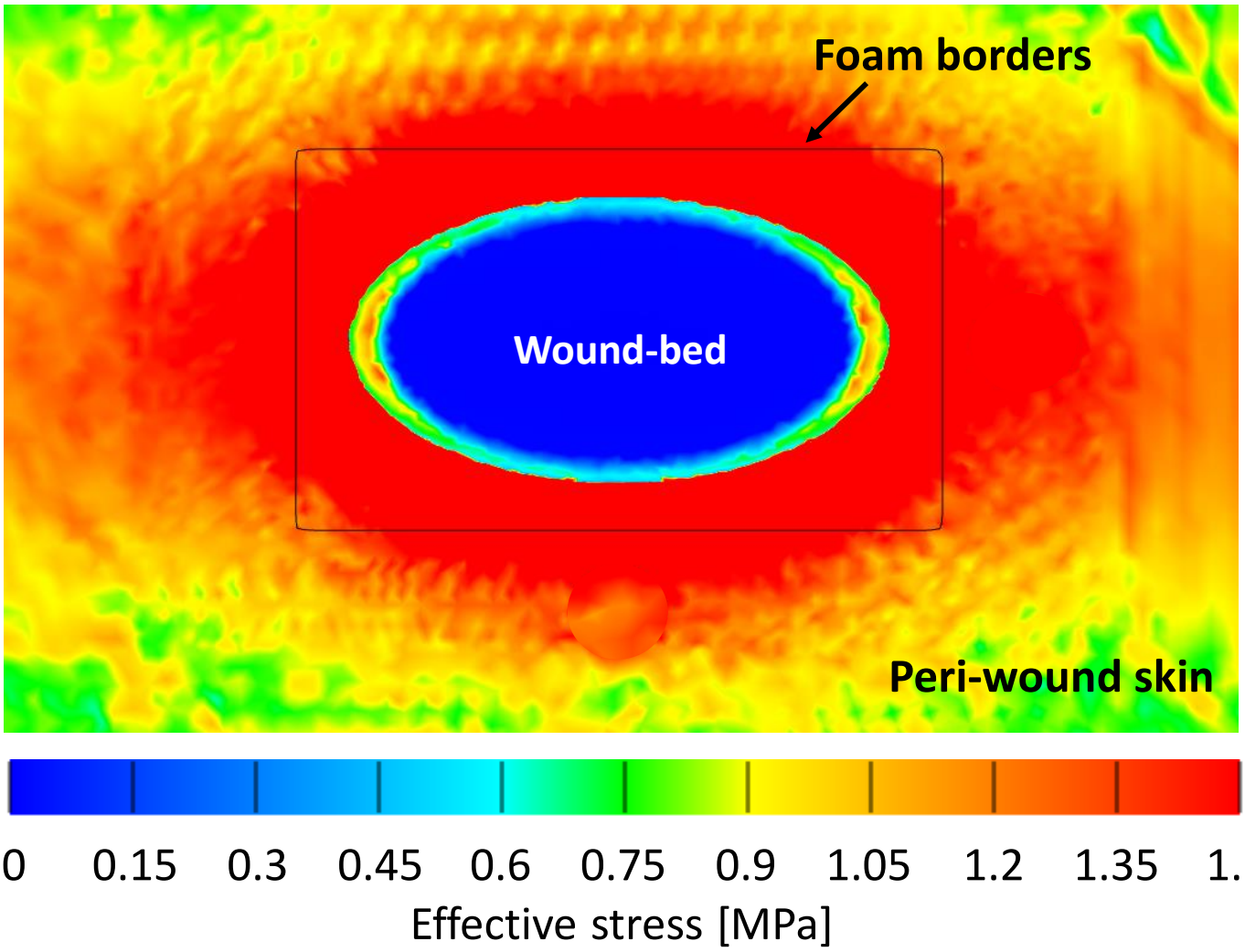
Foam borders
Wound-bed
Peri-wound skin
0
0.15
0.3
0.45
0.6
0.75
0.9
1.05
1.2
1.35
1.5
Effective stress [MPa]

(b)

Figure 2

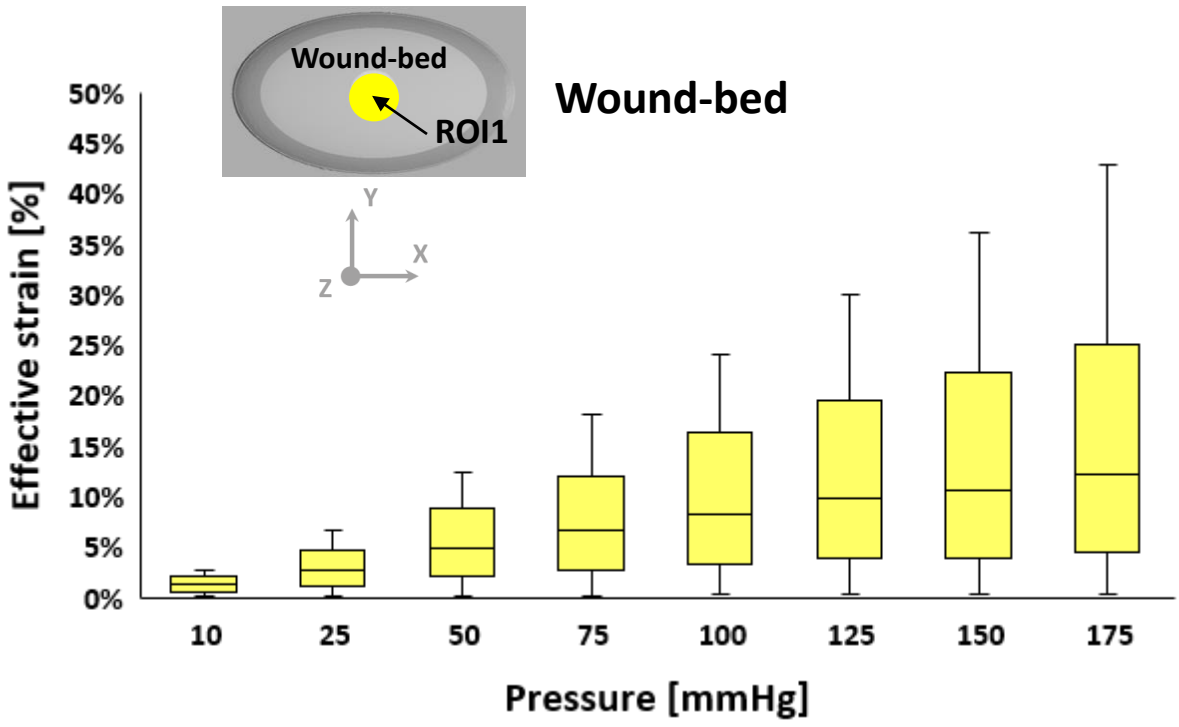
Wound-bed
ROI1
Wound-bed
Y
X
Z
50%
45%
40%
35%
30%
25%
20%
15%
10%
5%
0%
Effective strain [%]
10
25
50
75
100
125
150
175
Pressure [mmHg]

(a)

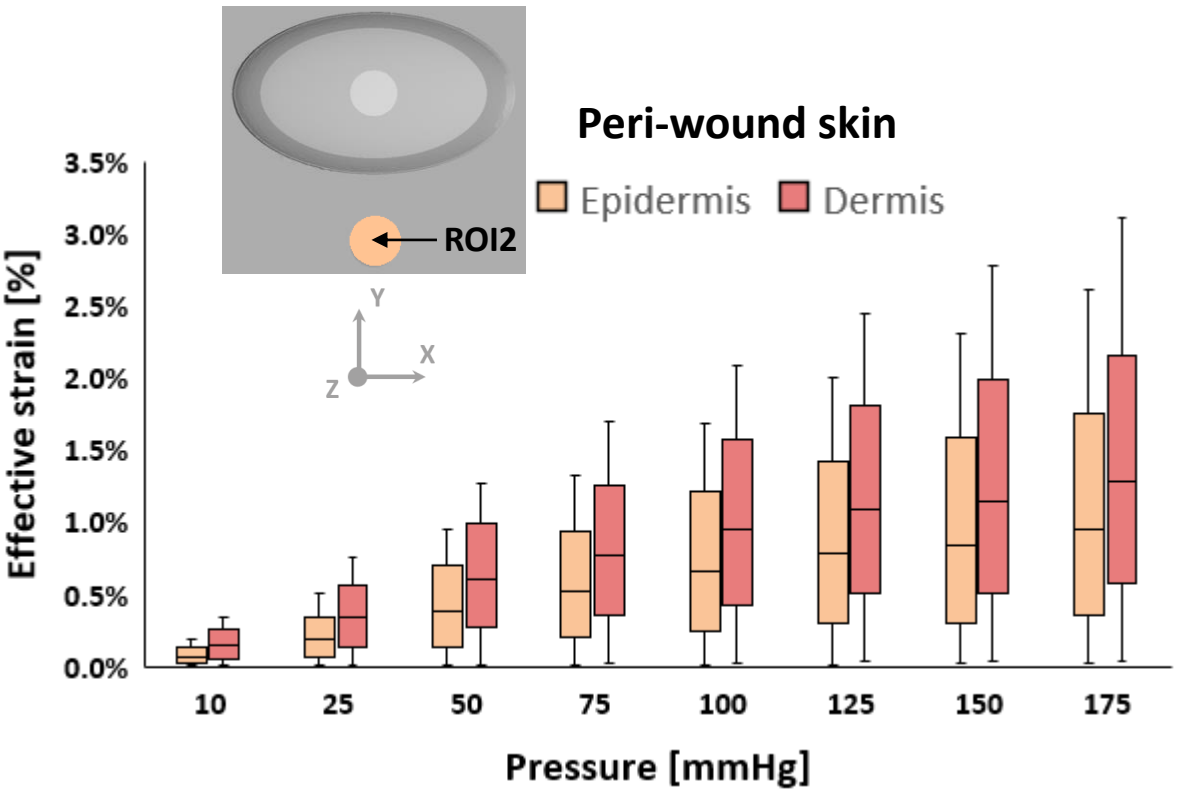
Peri-wound skin
Epidermis
Dermis
ROI2
Y
X
Z
3.5%
3.0%
2.5%
2.0%
1.5%
1.0%
0.5%
0.0%
Effective strain [%]
10
25
50
75
100
125
150
175
Pressure [mmHg]

(b)

Figure 3

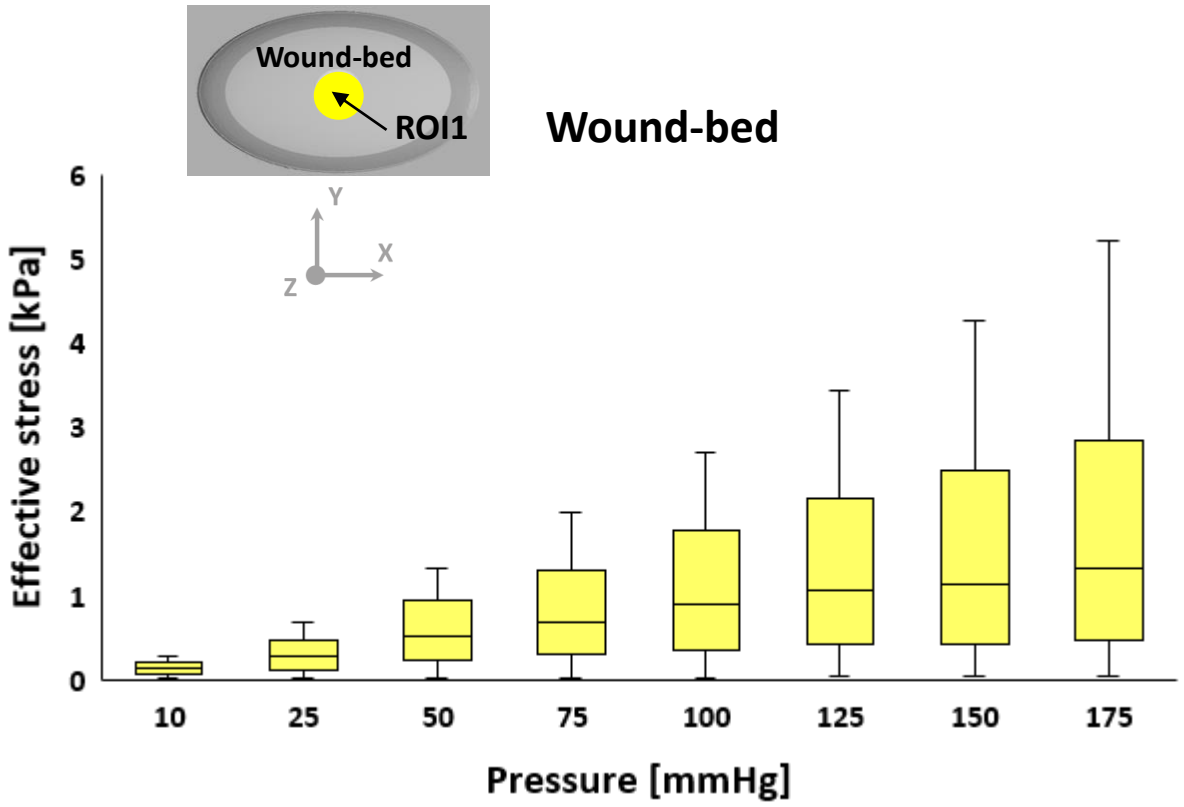
Wound-bed
ROI1
Wound-bed
Y
X
Z
Effective stress [kPa]
0
1
2
3
4
5
6
10
25
50
75
100
125
150
175
Pressure [mmHg]

(a)

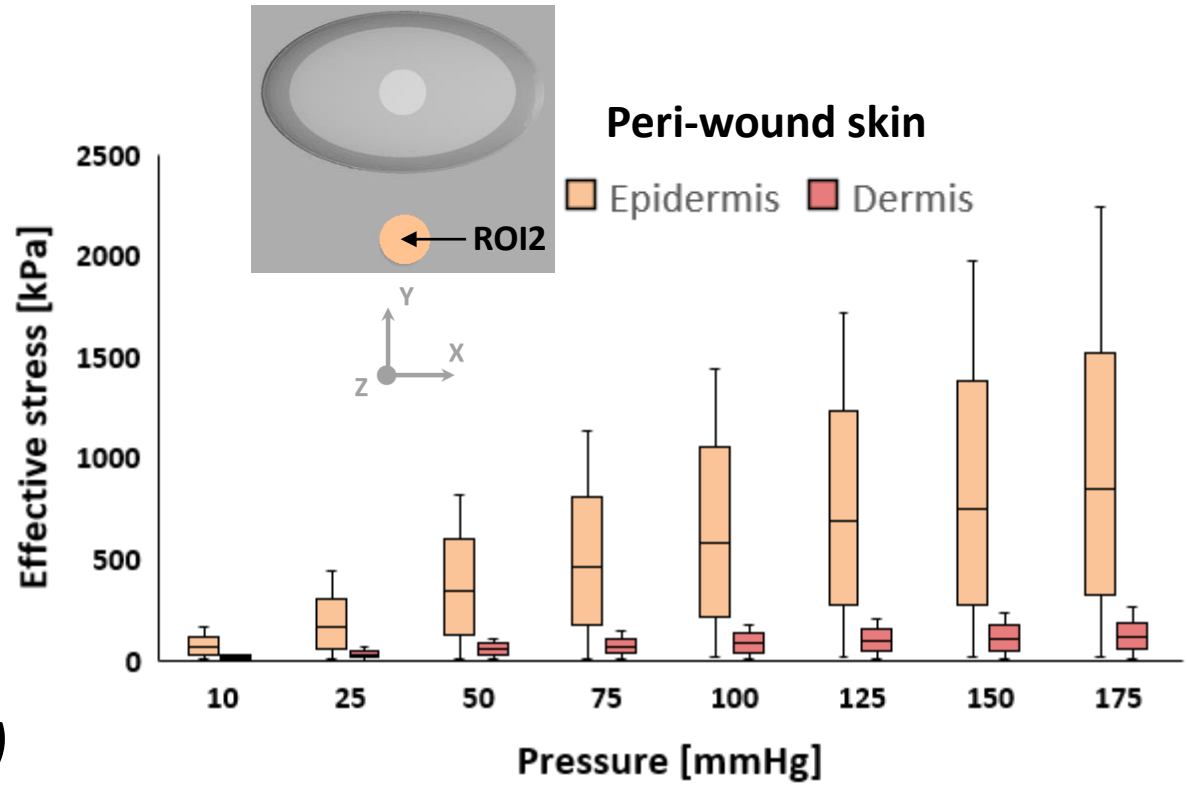
ROI2
Peri-wound skin
Epidermis
Dermis
Y
X
Z
Effective stress [kPa]
0
500
1000
1500
2000
2500
10
25
50
75
100
125
150
175
Pressure [mmHg]

(b)

Figure 4

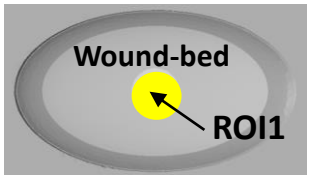
Wound-bed
ROI1

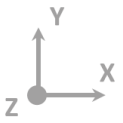
Y
X
Z

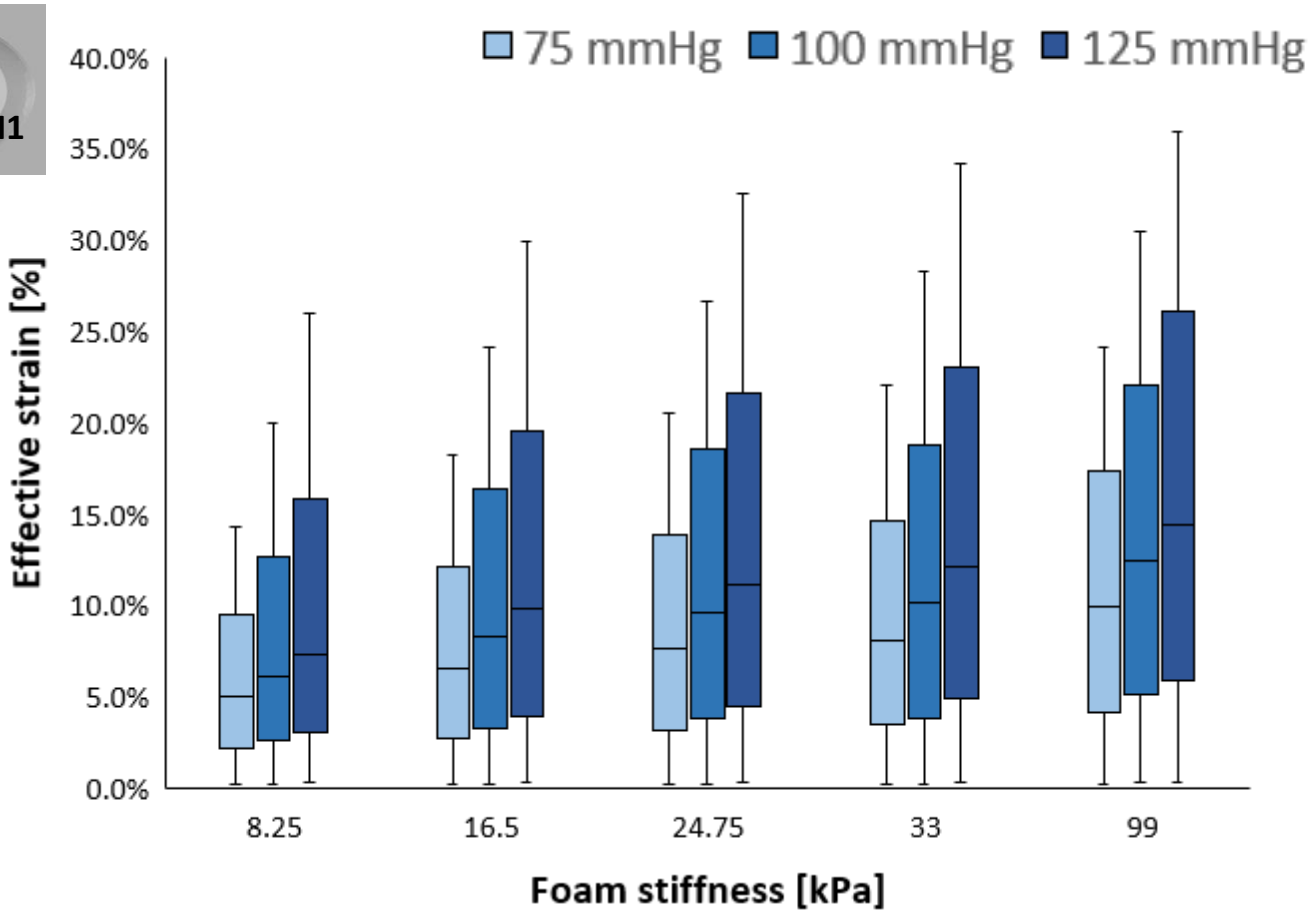
75 mmHg
100 mmHg
125 mmHg
Effective strain [%]
40.0%
35.0%
30.0%
25.0%
20.0%
15.0%
10.0%
5.0%
0.0%
8.25
16.5
24.75
33
99
Foam stiffness [kPa]

(a)

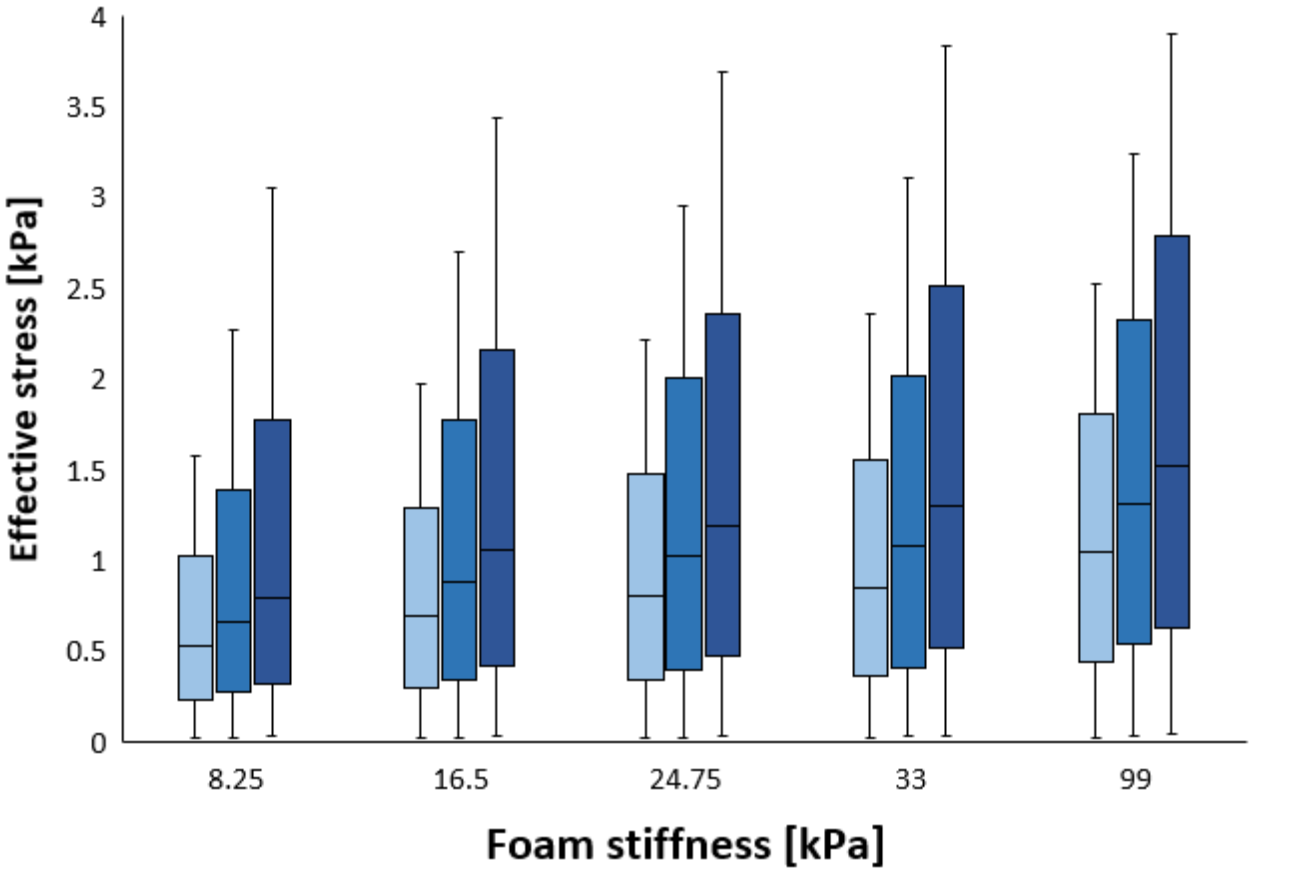
Effective stress [kPa]
4
3.5
3
2.5
2
1.5
1
0.5
0
8.25
16.5
24.75
33
99
Foam stiffness [kPa]

(b)

Figure 5

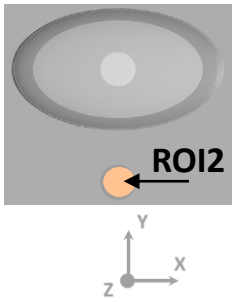
ROI2
Y
X
Z

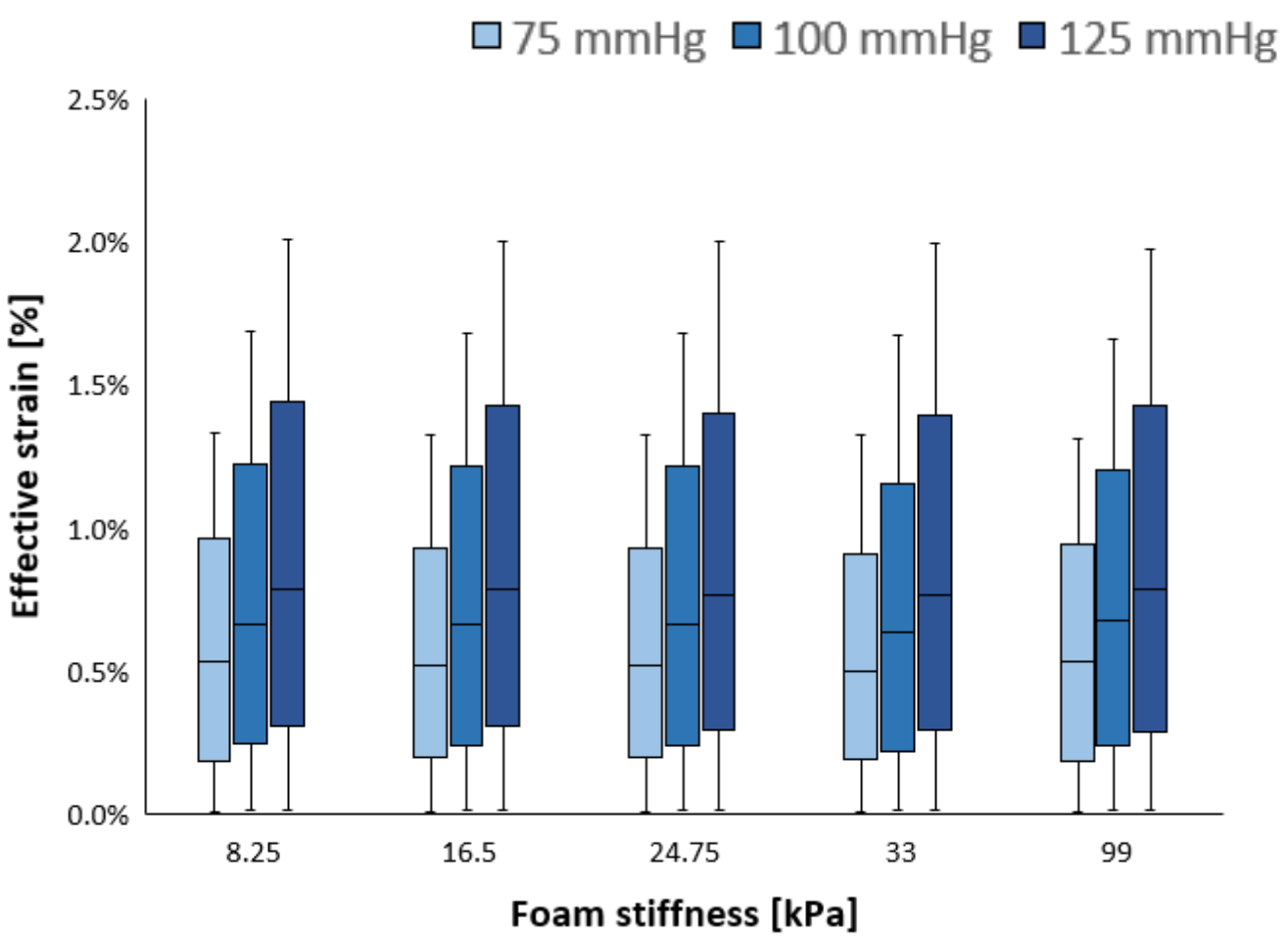
75 mmHg
100 mmHg
125 mmHg
2.5%
2.0%
1.5%
1.0%
0.5%
0.0%
Effective strain [%]
8.25
16.5
24.75
33
99
Foam stiffness [kPa]

(a)

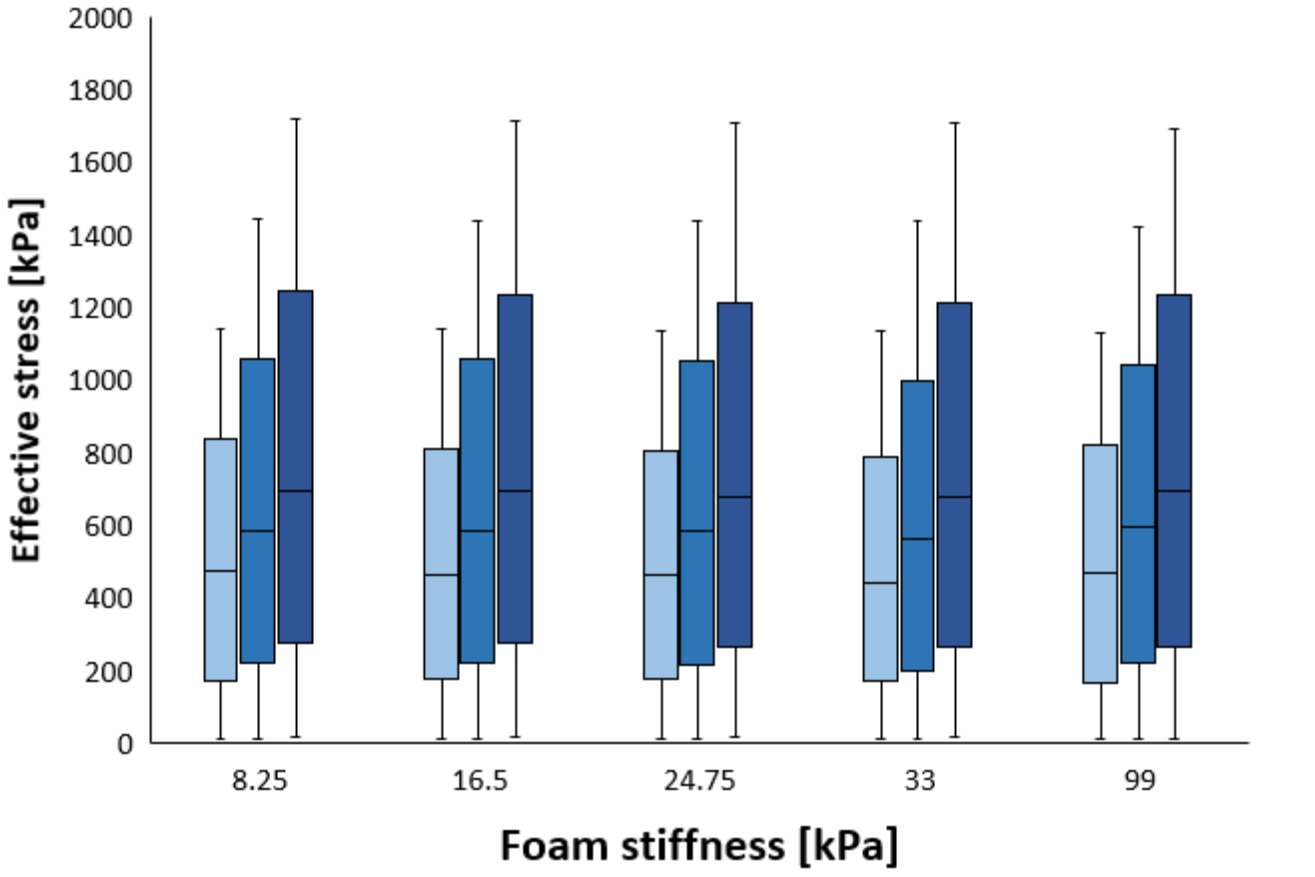
2000
1800
1600
1400
1200
1000
800
600
400
200
0
Effective stress [kPa]
8.25
16.5
24.75
33
99
Foam stiffness [kPa]

(b)

Figure 6

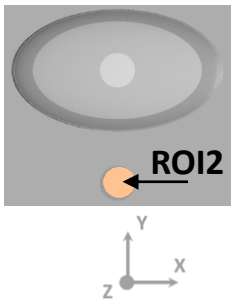
ROI2
Y
X
Z

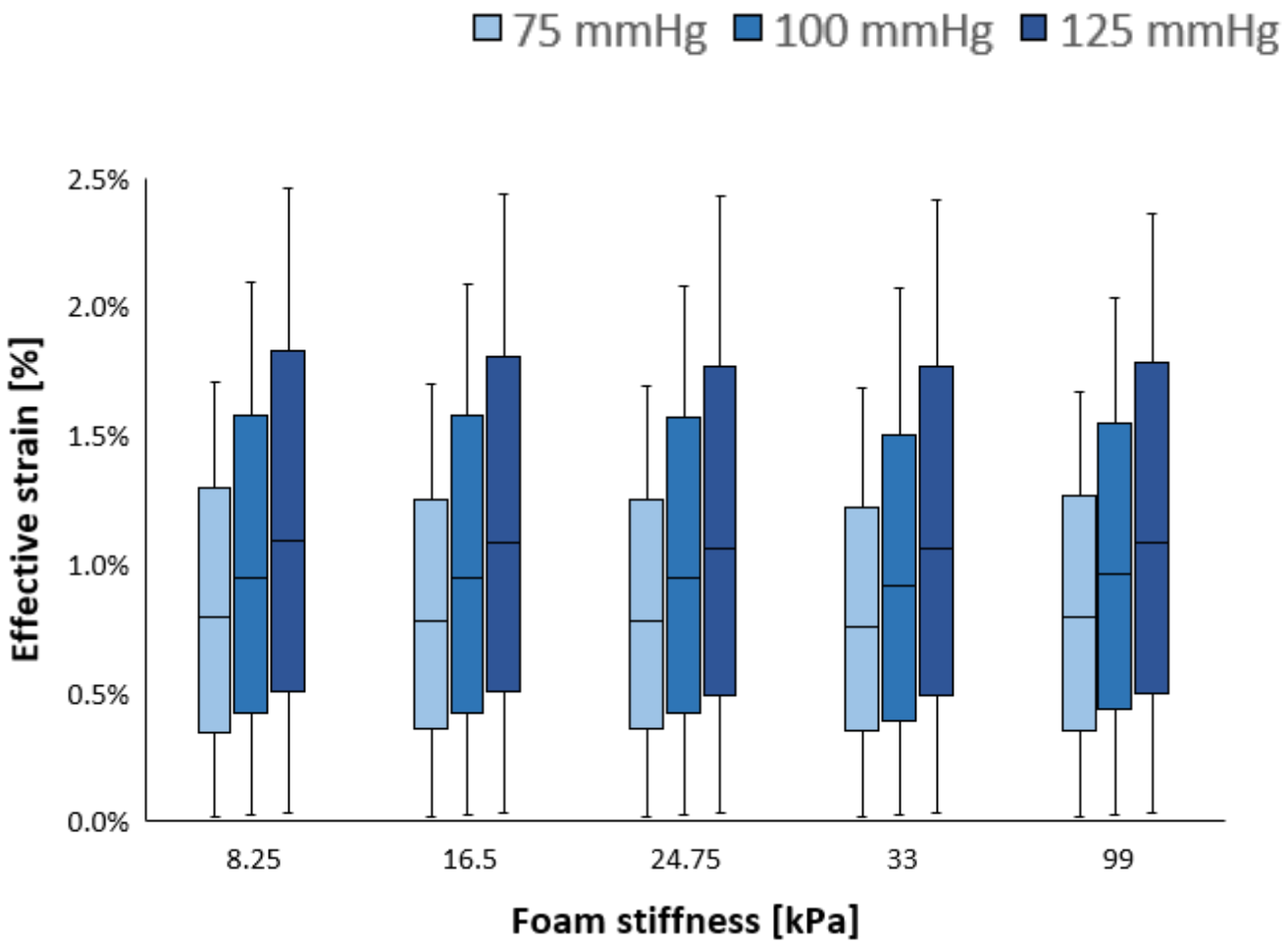
75 mmHg
100 mmHg
125 mmHg
Effective strain [%]
2.5%
2.0%
1.5%
1.0%
0.5%
0.0%
8.25
16.5
24.75
33
99
Foam stiffness [kPa]

(a)

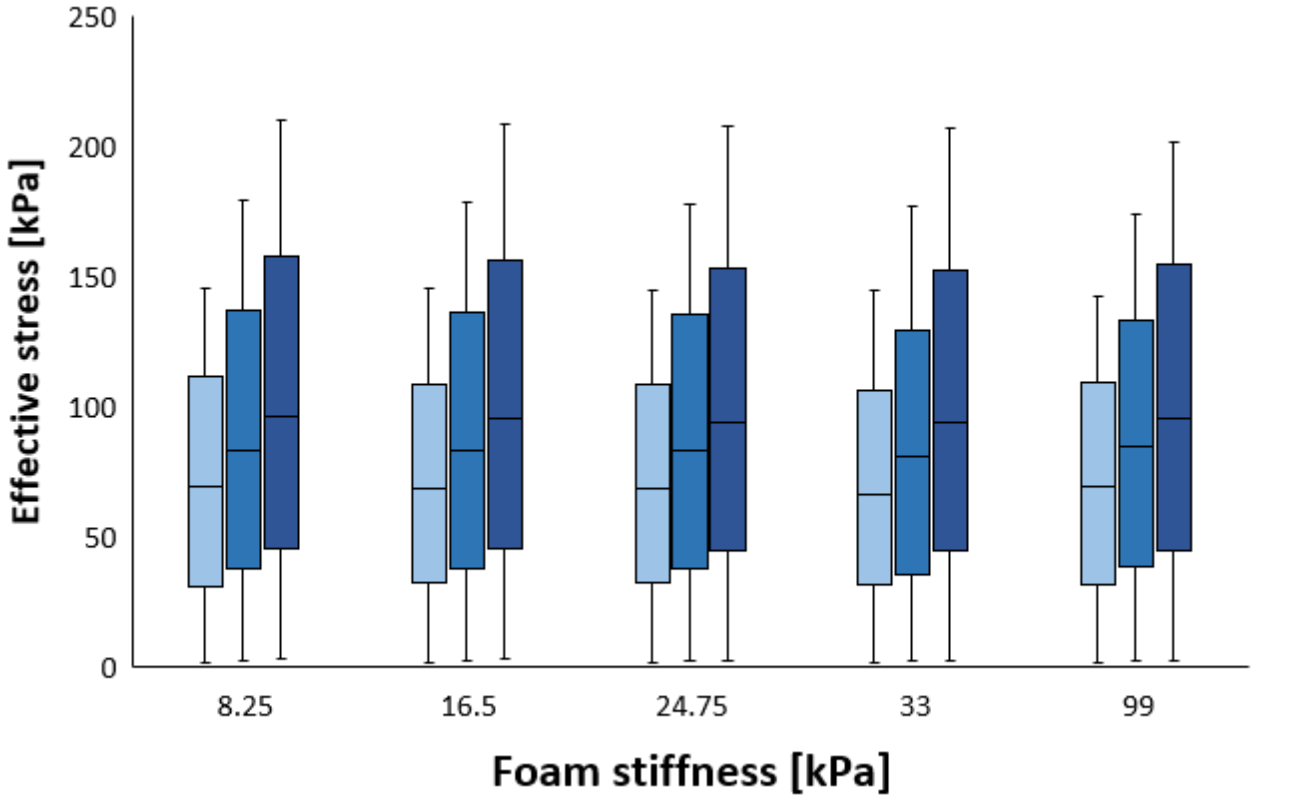
Effective stress [kPa]
250
200
150
100
50
0
8.25
16.5
24.75
33
99
Foam stiffness [kPa]

(b)

Figure 7